Cell

DNA Damage Regulates Alternative Splicing through Inhibition of RNA Polymerase II Elongation

Manuel J. Muñoz,[1] M. Soledad Pérez Santangelo,[1] Maria P. Paronetto,[3] Manuel de la Mata,[1] Federico Pelisch,[1] Stéphanie Boireau,[4] Kira Glover-Cutter,[2] Claudia Ben-Dov,[3] Matías Blaustein,[1] Juan J. Lozano,[3] Gregory Bird,[2] David Bentley,[2] Edouard Bertrand,[4] and Alberto R. Kornblihtt[1,*]

[1]Laboratorio de Fisiología y Biología Molecular, Departamento de Fisiología, Biología Molecular y Celular, IFIBYNE-CONICET, Facultad de Ciencias Exactas y Naturales, Universidad de Buenos Aires, Ciudad Universitaria, Pabellón 2, (C1428EHA) Buenos Aires, Argentina

[2]Department of Biochemistry and Molecular Genetics, University of Colorado Denver School of Medicine, MS8101, Aurora, CO 80045, USA

[3]Centre de Regulació Genòmica, Dr. Aiguader 88, 08003 Barcelona, Spain

[4]IGMM-CNRS UMR 5535, 1919, Route de Mende, 34293 Montpellier, France

*Correspondence: ark@fbmc.fcen.uba.ar

DOI 10.1016/j.cell.2009.03.010

SUMMARY

DNA damage induces apoptosis and many apoptotic genes are regulated via alternative splicing (AS), but little is known about the control mechanisms. Here we show that ultraviolet irradiation (UV) affects cotranscriptional AS in a p53-independent way, through the hyperphosphorylation of RNA polymerase II carboxy-terminal domain (CTD) and a subsequent inhibition of transcriptional elongation, estimated in vivo and in real time. Phosphomimetic CTD mutants not only display lower elongation but also duplicate the UV effect on AS. Consistently, non-phosphorylatable mutants prevent the UV effect. Apoptosis promoted by UV in cells lacking p53 is prevented when the change in AS of the apoptotic gene *bcl-x* is reverted, confirming the relevance of this mechanism. Splicing-sensitive microarrays revealed a significant overlap of the subsets of genes that have changed AS with UV and those that have reduced expression, suggesting that transcriptional coupling to AS is a key feature of the DNA-damage response.

INTRODUCTION

Alternative pre-mRNA splicing is more a rule than an exception because it is estimated to affect the expression of nearly 65% of human genes (Kim et al., 2007). The importance of alternative splicing (AS) is confirmed by findings that mutations that affect it are frequent in human hereditary disease (Cáceres and Kornblihtt, 2002) and because AS factors can be misregulated in cancer (Karni et al., 2007). It is now well established that splicing can be cotranscriptional and that AS regulation not only depends on the interaction of splicing factors, such as serine/arginine-rich proteins (SR proteins), with their target sequences in the pre-mRNA, but is also coupled to RNA polymerase II (Pol II) transcription, similar to what happens with other pre-mRNA processing reactions (Bentley, 2005; Kornblihtt et al., 2004; Maniatis and Reed, 2002). The ways in which transcription regulates AS involve both the association of splicing factors to the transcribing polymerase (recruitment coupling) (de la Mata and Kornblihtt, 2006) and modulation of Pol II elongation rates (kinetic coupling) (de la Mata et al., 2003).

AS seems to play a key role in the responses to DNA damage as suggested by the large number of apoptotic genes that are alternatively spliced, with often antagonistic roles of the isoforms generated. These include genes for several ligands, receptors, adaptor proteins, and regulators as well as members of the *Bcl-2*, caspase, and *p53* families (Schwerk and Schulze-Osthoff, 2005). Therefore, it is predicted that splicing factors and components of the transcription machinery, including Pol II itself, can be targets for intracellular cascades that link changes in splicing patterns to DNA-damage signals. These are particularly important for the variety of cellular responses they trigger, aimed at either repairing the damage or promoting apoptosis to prevent its expansion. DNA damage can be caused by endogenous reactive oxygen species and exogenous chemicals like DNA alkylating, intercalating, and crosslinking agents, as well as DNA topoisomerase inhibitors, some of which are widely used in the chemotherapy of cancer. DNA-damaging radiation includes X-rays, gamma rays, and ultraviolet irradiation (UV). The molecular responses elicited are complex and vary according to the nature of the lesion caused by the specific damaging agent (Skorski, 2002).

A few examples of UV-dependent regulation of AS have been reported, but the precise underlying mechanism is not known (Chandler et al., 2006; Katzenberger et al., 2006; Nicholls et al., 2004). More information is available on the effects of UV treatment on other aspects of mRNA biogenesis and processing. Inhibition of transcriptional initiation by Pol II was reported to follow UV treatment (Rockx et al., 2000) and Pol II was demonstrated to stall at the photolesions themselves (Damsma et al., 2007). UV inhibits mRNA 3′-end formation, via a mechanism

involving the tumor suppressors BRCA-1 and BARD-1. UV-mediated DNA damage stabilizes BRCA-1/BARD-1 complexes that sequester the cleavage stimulation factor CstF-50. In parallel, BRCA-1/BARD-1 complexes display an E3 ubiquitin ligase activity that specifically ubiquitylates the phosphorylated form of Pol II (Pol IIO), inducing its degradation by the proteasome. Because Pol IIO was shown to be necessary for efficient 3′-end processing (Hirose and Manley, 1998), these results were interpreted as an adaptive response in which degradation of stalled Pol IIO would inhibit the coupled transcription-RNA processing machinery and facilitate repair (Kleiman and Manley, 2001; Kleiman et al., 2005). Although other interpretations are possible, these findings highlight the importance of investigating the transcription/processing coupling as a putative target of DNA-damage signaling.

In this study we use the AS of the EDI exon (extra domain I, a.k.a. EDA or EIIIA) of human fibronectin (FN) as a coupling model. In fact, EDI AS is not only controlled by the SR proteins SF2/ASF and SRp20 but is also modulated by promoter occupation (Cramer et al., 1999), transcriptional elongation (de la Mata et al., 2003; Kadener et al., 2001), and factor recruitment to the carboxy-terminal domain (CTD) of Pol II (de la Mata and Kornblihtt, 2006). We found that low doses of UV upregulate the inclusion of the EDI exon and the proapoptotic mRNA isoforms of Bcl-x and caspase 9 (C9). AS is equally affected in transcripts of DNA templates transfected before or after UV treatment of cells, which indicates that the effect is not due to the actual damage of the DNA template in *cis*. Instead, UV triggers a systemic mechanism involving the kinetic coupling between transcription and splicing affecting cotranscriptional AS. Using fluorescence recovery after photobleaching (FRAP) to measure Pol II elongation in vivo, we demonstrate that the mechanism involves inhibition of Pol II elongation through CTD hyperphosphorylation. Unlike other cell responses to UV, the effects on AS are not mediated by the transcription factor p53 and, moreover, apoptosis promoted by UV in cells lacking this factor is prevented when the change in Bcl-x AS ratio is reverted. Finally, using a splicing-sensitive human microarray platform, we found that the subset of genes that change AS with UV is highly increased among the genes that also downregulate its expression, suggesting that modulation of AS through its coupling with transcription is a key feature of the DNA-damage response.

RESULTS AND DISCUSSION

UV Treatment Affects AS

Irradiation of cells in culture with low doses of 254 nm UV (UVC, 10–50 J/m^2) caused a 2.5-fold increase in the inclusion levels of the EDI alternative cassette exon into endogenous FN mRNA (Figure 1A, lanes 1 and 2). The effect is not restricted to FN splicing or to cassette exons because UV also affects the splicing pattern of the *bcl-x* gene (lanes 3 and 4) by increasing the relative proportion of the short mRNA isoform resulting from two competing 5′ splice sites. The relative proportion of the long isoform of C9 mRNA is also increased by UV treatment (lanes 5 and 6).

Similar effects are observed when cells are treated with cisplatin (Figure S1 available online), an anticancer drug that damages DNA by forming mainly 1,2-d(GpG) intrastrand cross-links, which differ from the intrastrand cyclobutane pyrimidine dimers (CPD) and 6-4 photoproducts (6-4PP) provoked by UV.

AS patterns of transfected minigenes are also affected by UV, and the fold increase observed is comparable with the different promoters analyzed (Figure 1B). As expected, the magnitude of changes observed when using transfected minigenes is higher compared with that of endogenous genes because we are looking at the effects of UV on de novo mRNA synthesis. Changes in mRNA isoform abundances could be caused by changes in AS or differential isoform degradation. Figure 1C shows that UV is acting on AS of the three genes studied here, and not on degradation, because its effect was abolished when transcription was blocked with actinomycin D before irradiation.

In view of these results, we decided to investigate the mechanism (Figures 2–5), the biological implications (Figure 6), and the generality (Figure 7) of the UV effect on AS.

DNA Damage In *cis* Is Not Necessary for the UV Effect

The similar effects of UV and cisplatin indicate that the changes in AS are triggered by DNA damage. Moreover, lesions in the DNA template are known to block transcription elongation and lead to Pol II stalling in *cis* (Damsma et al., 2007). Because stalling of Pol II can cause changes in AS through kinetic coupling (Batsche et al., 2006), we decided to investigate whether the UV effect on AS was caused by lesions on the actual DNA template in *cis*. For this, we compared the effects of UV treatment performed either after (AT) or before (BT) transfecting an EDI reporter minigene, with respect to nonirradiated cells (NI). Surprisingly, UV caused a similar increase in EDI exon inclusion (approximately 8-fold) independent of the relative order of transfection and irradiation (Figure 2A). This indicates that damage of the actual template in *cis* is not necessary for the observed effect of UV on AS.

The UV Effect Is Independent of p53

If damage is causative it should be through evoking systemic responses related to stress signaling that might affect the properties of nuclear proteins involved in transcription and/or splicing. Among these, the phosphorylation of the tumor suppressor p53 is of major importance in the response to genotoxic agents (Efeyan and Serrano, 2007). Phosphorylated p53 activates transcription of numerous genes involved in cell cycle progression and apoptosis. The relevance of p53 is dramatically illustrated by its need for the most conspicuous effect of UV in animals: the suntan response. Indeed, mice lacking p53 do not display hyperpigmentation after UV treatment because transcription of the proopiomelanocortin gene requires p53 (Cui et al., 2007).

Despite its importance, p53 is not necessary for the UV effect on AS of FN, Bcl-x, and C9 genes because it takes place in Hep3B cells that are considered to be p53 null (IARC TP53 Mutation Database). To confirm this observation, we used two isogenic human cell lines (HCT116 p53$^{+/+}$ and HCT116 p53$^{-/-}$), differing by the knockout of the p53 gene. Indeed, the effects of UV are still observed in p53$^{-/-}$ HCT116 cells for the three genes analyzed (Figures 2B–2D). Caffeine is a specific inhibitor of ATM and ATR, the protein kinases that phosphorylate p53 in response

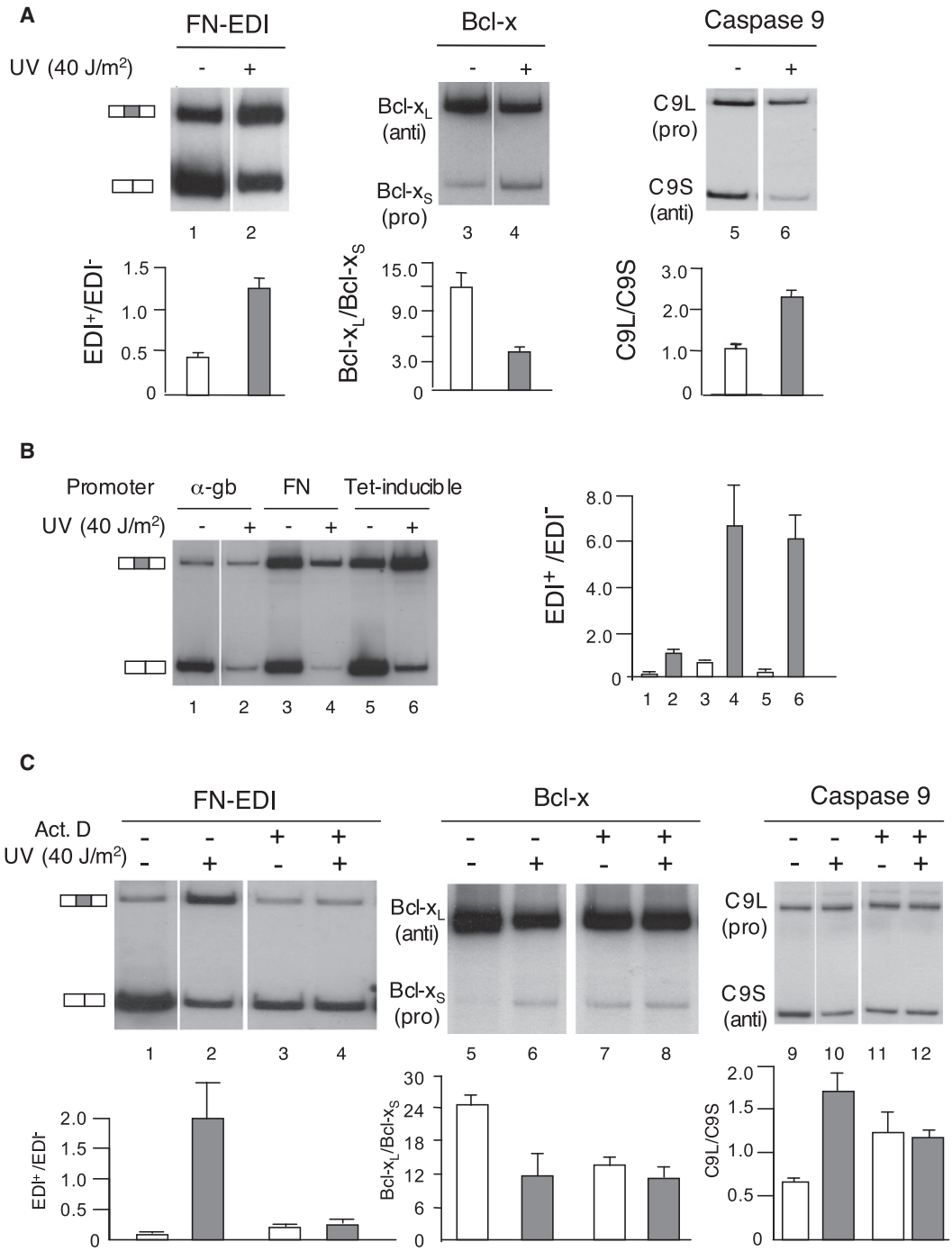

Figure 1. UV Affects AS

(A) UV (UVC, 254 nm) increases the inclusion of the EDI exon into endogenous FN mRNA (lanes 1 and 2) and the relative proportions of the proapoptotic (pro) isoforms of Bcl-x (lanes 3 and 4) and C9 (lanes 5 and 6) in Hep3B cells. Anti, antiapoptotic.

(B) UVC increases the inclusion of EDI in mRNAs expressed from minigenes. Hep3B cells were transfected with EDI reporter minigenes with different promoters: FN, fibronectin; α-gb, alpha globin; Tet-inducible, Tet-off promoter.

(C) In the presence of actinomycin D (added 1 hr before irradiation), there is no change in the proportions of EDI, Bcl-x, and C9 AS isoforms upon UV treatment. In all experiments, cells were harvested 15 hr after irradiation. AS of FN, Bcl-x, and C9 mRNA isoforms were assessed by radioactive RT-PCR with specific pairs of primers for the endogenous (FN, Bcl-x, and C9) or minigene-derived (FN) mRNAs, followed by electrophoresis in native polyacrylamide gels as described in Experimental Procedures. Means and standard deviations (SD) are shown (n = 3).

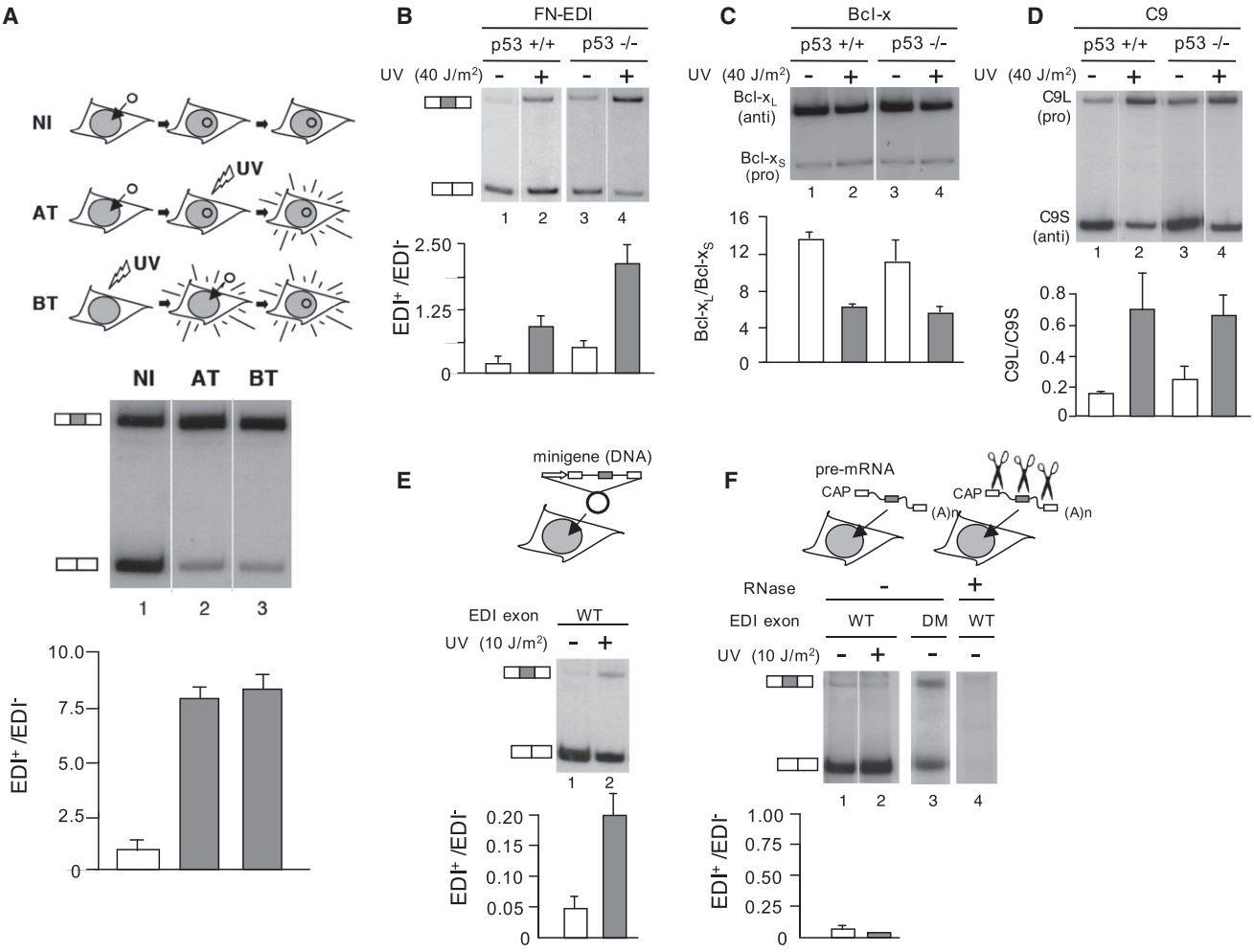

Figure 2. UV-Induced DNA Damage Affects Cotranscriptional AS through a Systemic and p53-Independent Mechanism

(A) Hep3B cells were transfected with the FN EDI reporter minigene. Cells were either not irradiated (NI, lane 1), irradiated after transfection (AT, lane 2), or irradiated before transfection (BT, lane 3) with UVC at 40 J/m^2, and harvested 15 hr later.

(B–D) The UV effect on AS is observed independent of p53. Wild-type HCT116 (lanes 1 and 2) or p53$^{-/-}$ (lanes 3 and 4) cells were irradiated (lanes 2 and 4) o not irradiated (lanes 1 and 3) with UVC at 40 J/m^2. AS was assessed by RT-PCR as in Figure 1 for FN-EDI (B), Bcl-x (C), and C9 (D).

(E) The UV effect is observed when both cotranscriptional and posttranscriptional splicing can occur by transfecting the α-gb-promoter reporter minigene (lanes 1 and 2).

(F) The UV effect is not observed when only posttranscriptional splicing can take place upon direct transfection of an in-vitro-synthesized pre-mRNA. The capped and polyadenylated pre-mRNAs made in vitro, corresponding to wt (lanes 1, 2, and 4) minigenes used in (A), were transfected into Hep3B cells with (only lane 4) or without pretreatment with RNase A. Lane 3 shows transfection with in vitro synthesized, capped, and polyadenylated pre-mRNA from a minigene (DM) that displays high levels of EDI inclusion due to the optimization of EDI 3′ splice site (Fededa et al., 2005). Cells were irradiated (only lane 2) with UVC at 10 J/m^2 and harvested 20 hr after irradiation. AS was assessed by radioactive RT-PCR as in Figure 1 with specific primers (see Experimental Procedures). Means and SD are shown (n = 3).

to DNA damage. In agreement with the p53$^{-/-}$ cell results, caffeine does not alter the UV effect on AS (Figure S2A). Similar results were reported by Chandler et al. (2006) on changes in MDM2 mRNA isoforms after UV treatment.

The UV Effect Is Not Linked to Defects in 3′-End Processing

A p53-independent pathway triggered by DNA damage that targets pre-mRNA processing involves the above-mentioned stabilization of BRCA1/BARD1 complexes induced by DNA damage, resulting in inhibition of mRNA 3′-end formation (Kleiman and Manley, 2001). Because splicing and 3′-end formation are coupled (Maniatis and Reed, 2002), we wondered whether the UV effect on AS was indirectly caused by inhibition of pre-mRNA cleavage and polyadenylation. Removal of the poly(A) signal from the template did not abrogate the UV effect on AS (Figure S2B). Control experiments using oligo-dT affinity chromatography indicate that deletion of the poly(A) signal inhibits polyadenylation by more than 80% (bottom chart). These experiments, together with evidence that knock down of BRCA1 and BARD1 does not affect the UV effect (Figure S2C), rule out the polyadenylation pathway.

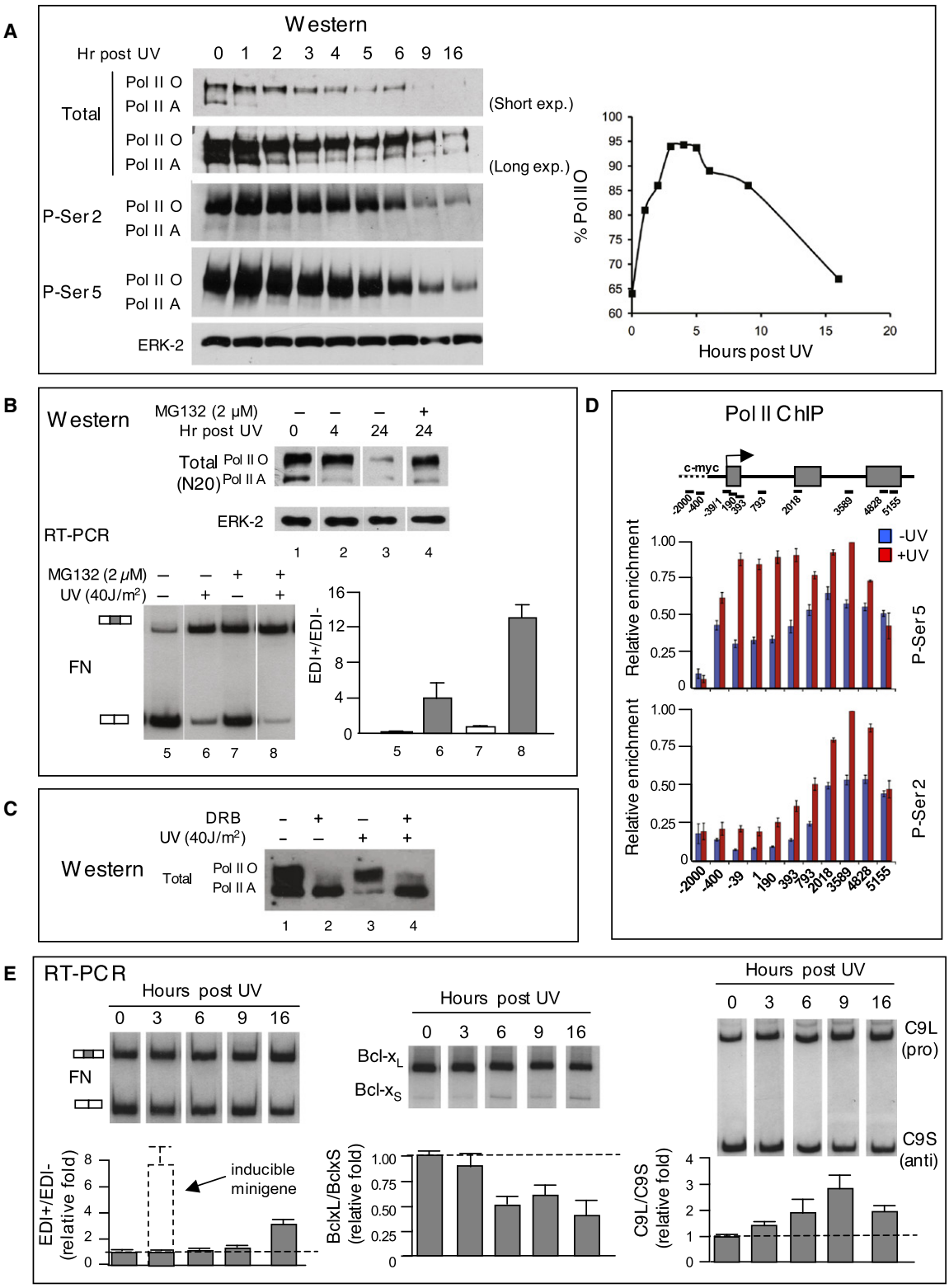

Figure 3. The UV Effect and CTD Phosphorylation

(A) Western blots for Pol IIO (hyperphosphorylated) and pol(A) (hypophosphorylated) forms from Hep3B cells at different times after UV (20 J/m^2) treatment, using antibodies to total Pol II (N20, Santa Cruz Biotechnology) or specific to CTD phosphorylated at Ser2 (H5, Covance) or Ser5 (H14, Covance). Loading control was performed with an antibody to Erk2 (Santa Cruz Biotechnology). Quantification of the Pol IIO percent intensities is shown in the plot (right).

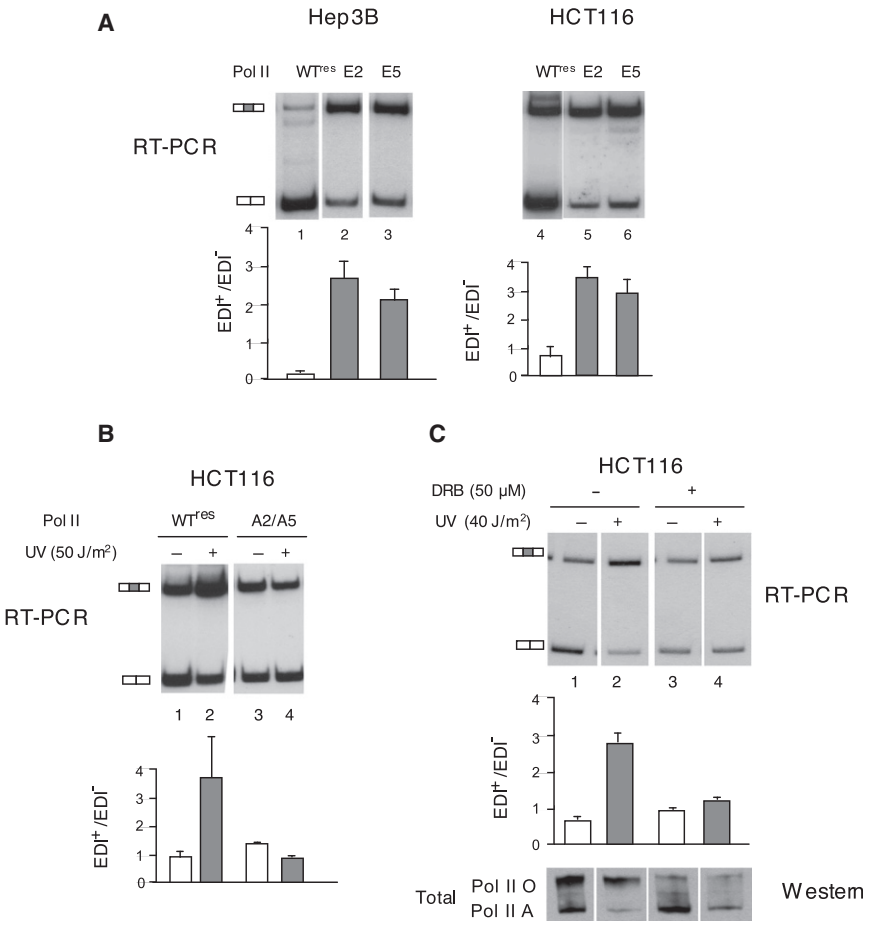

Figure 4. Phosphomimetic CTD Mutants Duplicate whereas Nonphosphorylatable CTD Abrogates the UV Effect on AS

(A) Human Pol II mutants carrying in their CTD repeats glutamic acid residues in replacement of serines 2 (E2, lanes 2 and 5) or 5 (E5, lanes 3 and 6) duplicate the effects of UV on AS. Hep3B (lanes 1–3) or HCT116 (lanes 4–6) cells were transfected with α-amanitin-resistant wt (WT^{res}) (lanes 1 and 4) or mutant Pol II large subunits together with a reporter minigene for EDI AS and treated with α-manitin as described elsewhere (de la Mata and Kornblihtt, 2006).

(B) α-Amanitin-resistant polymerases with wt CTD (lanes 1 and 2) or carrying alanines instead of serines at positions 2 and 5 (lanes 3 and 4) were transfected in HCT116 cells and irradiated (lanes 2 and 4) or not irradiated (lanes 1 and 3).

(C) DRB has no effect on basal EDI inclusion in HCT116 cells but inhibits its stimulation by UV treatment. RT-PCR (top) and total Pol II western blot (N20, bottom) of cells transfected with the Tet-inducible FN minigene, irradiated with UV, and treated with DRB as indicated. For all RT-PCRs, means and SD are shown (n = 3).

The UV Effect Is Not Caused by Changes in SR Protein Localization

UV treatment was previously shown to decrease the nuclear concentration of splicing factors such as hSlu7 (Shomron et al., 2005) and hnRNPA1 (van der Houven van Oordt et al., 2000) by promoting their shuttling to the cytoplasm, which in turn affected AS. However, the UV doses used in these reports, ranging from 200 to several thousand J/m^2, are much higher than the ones used here (10–50 J/m^2). The SR proteins SRp20, SF2/ASF, and SC35, which regulate EDI exon inclusion, display different patterns of intranuclear localization. Although SRp20 has a nucleoplasmic homogeneous distribution, SF2/ASF and SC35 concentrate in "speckles." At our doses, no changes in the localization of these splicing factors were observed (Figure S3).

UV Affects Cotranscriptional but Not Posttranscriptional AS

Splicing can occur both cotranscriptionally and posttranscriptionally. Whereas UV stimulation of EDI exon inclusion is observed in transfections with reporter minigenes (DNA) that allow for cotranscriptional splicing (Figures 1B, 2A, and 2E), transfection of in-vitro-transcribed pre-mRNA, a strategy used before to look at posttranscriptional splicing (Robson-Dixon and Garcia-Blanco, 2004), allows for AS, but no UV effect is observed (Figure 2F, lanes 1 and 2). This indicates that the UV effect on EDI requires cotranscriptional splicing. Different experimental controls support this conclusion. The sequences of the pre-mRNAs made in vitro or transcribed from the transfected reporter minigene are identical. The in-vitro-transcribed pre-mRNA was capped and polyadenylated also in vitro before transfection, to reduce its degradation and improve its processing once transfected. Using capped and polyadenylated

(B) The UV effect is not due to Pol II degradation. Top: Total Pol II western blot (N20) of Hep3B cells at different times after UV treatment (20 J/m^2). In lane 4, the proteasome inhibitor MG132 (2 μM) was added to the cells before irradiation. Bottom: Cells were transfected with a Tet-inducible FN minigene in the presence of tetracycline. Twelve hours later, MG132 (2 μM) was added (lanes 7 and 8), and 1 hr later the cells were irradiated (lanes 6 and 8) and tetracycline was washed out to allow transcription for 4 hr. Cells were then harvested, RNA purified, and EDI AS assessed as in Figure 1. Means and SD are shown (n = 3).

(C) Total Pol II western blot (N20) of Hep3B cells, nonirradiated (lanes 1 and 2) or 4 hr after UV treatment (40 J/m^2) (lanes 3 and 4). In lanes 2 and 4, the Cdk-9 inhibitor DRB (50 μM) was added to the cells 3 hr before irradiation.

(D) UV treatment promotes CTD phosphorylation at both Ser5 and Ser2 of Pol II engaged in transcription. Top: Diagram of the human *myc* gene. Positions of the real-time PCR products are indicated relative to *myc* P2 start site. Bottom: ChIP analysis. ChIP signals for CTD P-Ser5 and P-Ser2, relative to total Pol II, are shown for nonirradiated (blue) or UV-treated (red) HCT116 cells. Means and SD are shown (n = 4 for the P-Ser5 graph and n = 3 for the P- Ser2 ratio graph).

(E) Time course of the changes in AS for endogenous FN EDI (left), Bcl-x (center), and C9 (right) in Hep3B cells at different times after UV treatment (20 J/m^2). Means and SD are shown (n = 3).

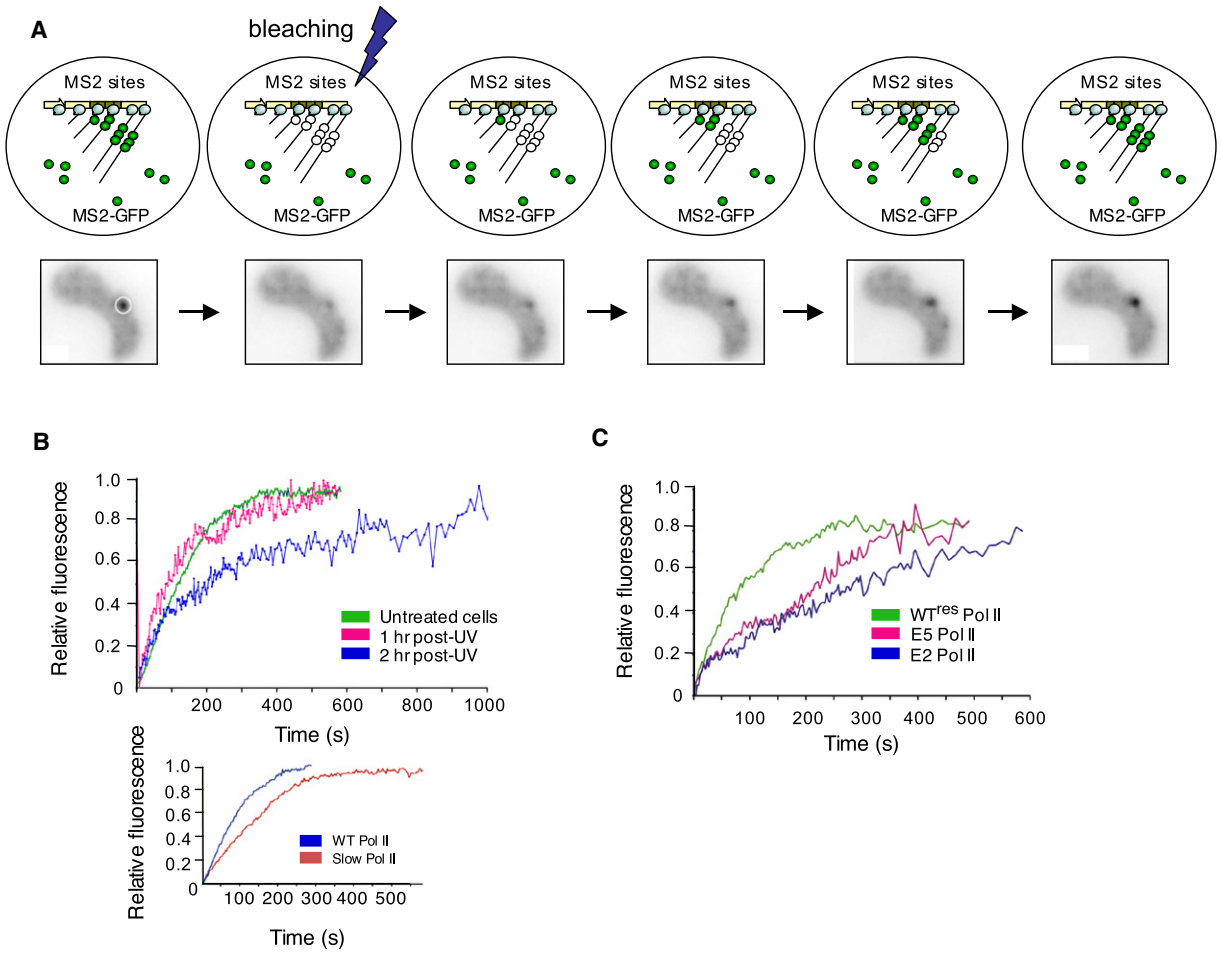

Figure 5. UV Treatment Inhibits Transcriptional Elongation In Vivo

(A) Schematic diagram of the kinetics of mRNA biogenesis in vivo and in real time using FRAP. Micrographs of a nucleus displaying fluorescence intensities at a single transcription focus before bleaching and during recovery are shown underneath.

(B) ExoLong cells (Boireau et al., 2007) were transfected with vectors expressing MS2-GFP 16 hr before irradiation or not with UVC at 40 J/m^2. FRAP was carried out as described in Experimental Procedures. FRAP curves were obtained by tracking transcription sites in three dimensions for 15 min, with a wide-field microscope. The recovery curve at the bottom corresponds to a control with a slow mutant of human RNA polymerase II as used in Boireau et al. (2007).

(C) Kinetics of mRNA biogenesis in vivo and in real time using FRAP as in (B). ExoShort cells were transfected with vectors expressing MS2-GFP and the WT^{res} or mutant (E2 or E5) RNA polymerases, and treated with α-amanitin before FRAP.

radioactive pre-mRNA, we determined that 66% of the transfected precursor accumulates in the nuclear fraction, showing a splicing efficiency similar to the one estimated for the splicing in vitro of precursors with long introns (Lazarev and Manley, 2007). Most importantly, transfection of an in-vitro-synthesized pre-mRNA with a mutation that optimizes the suboptimal 3′ splice site of the EDI exon allows for high EDI inclusion levels (Figure 2F, lane 3), indicating that the low EDI inclusion levels observed upon UV treatment (lane 2) are not the result of an intrinsic impairment of the RNA transfection system. Treatment of the in vitro synthesized pre-mRNA with RNase A previous to transfection shows no bona fide mRNA products in the transfected cells (lane 4), reassuring that the mature mRNAs can only result from the splicing of the transfected precursor RNA.

The UV Effect and Pol II CTD Phosphorylation

The strict need for cotranscriptionality for the UV effect on EDI splicing drew our attention to the modifications and properties induced by UV on Pol II. Pol II transcription is inhibited following DNA damage (Rockx et al., 2000). Two covalent modifications are associated with this phenomenon. Both UV and cisplatin induce first the hyperphosphorylation of Pol II's CTD, followed by ubiquitylation of the large subunit at non-CTD residues. Ubiquitylation in turn accelerates proteasome-dependent degradation (Luo et al., 2001; Somesh et al., 2005). Western blots in Figure 3A using specific antibodies for total Pol II (N20) or Pol II phosphorylated at Ser2 (H5) or Ser5 (H14) illustrate the time course of hyperphosphorylation and degradation in our system. Starting with a 65% of Pol IIO, 3 hr after UV exposure the maximum phosphorylation level is achieved (95%) and

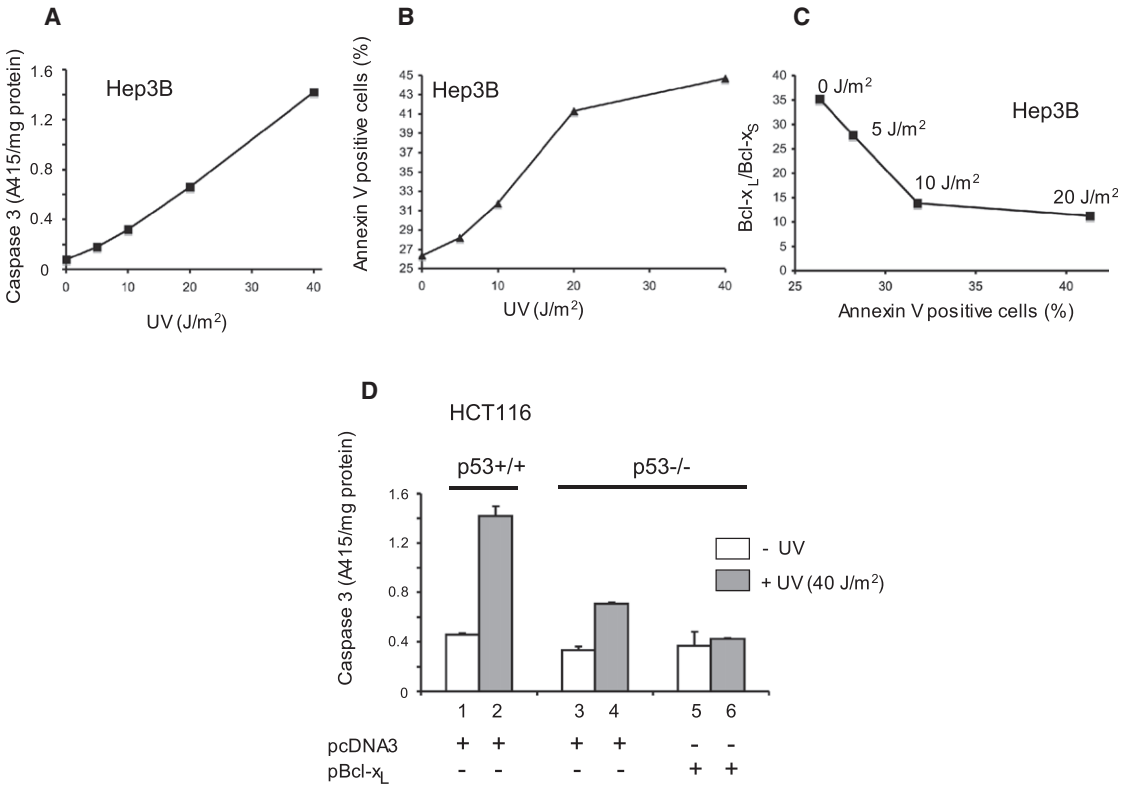

Figure 6. The p53-Independent Apoptosis Is Dependent on Bcl-x AS Ratio

(A and B) Hep3B cells were irradiated with different doses of UV and 18 hr later caspase 3 activity (A) or the percentage of annexin-V-positive cells (B) was determined.

(C) A negative correlation between the Bcl-x_L/Bcl-x_S ratio and the number of apoptotic cells is observed when Hep3B cells are irradiated with different UV doses and harvested 18 hr later.

(D) The UV-induced p53-independent apoptosis, measured as caspase 3 activity, is abrogated by Bcl-x_L overexpression. As a control for UV-induced caspase 3 activity, HCT116 $p53^{+/+}$ cells (lanes 1 and 2) were irradiated with 40 J/m^2 (lane 2) or not (lane 1). HCT116 $p53^{-/-}$ cells (lanes 3 to 6) were irradiated (lanes 4 and 6) or not (lanes 3 and 5) and transfected with a control plasmid (lanes 3 and 4) or a Bcl-x_L expression plasmid (lanes 5 and 6). Caspase 3 activity was determined 18 hr later. Means and SD are shown (n = 3).

degradation becomes evident. This percentage of hyperphosphorylation persists for 2 more hours and then decays because the hyperphosphorylated form IIO is preferentially degraded. At 16 hr degradation is maximal and the percentage of hyperphosphorylation falls back to 65%. Both Ser2 and Ser5 are hyperphosphorylated with no evident preference. Ubiquitylation is evidenced because degradation is prevented by the proteasome inhibitor MG132 (Figure 4B, top panel). How do these Pol II modifications correlate with the UV effect on AS? Three facts suggest that the effect on splicing is linked to Pol II hyperphosphorylation and not to its degradation. First, 3 hr after UV treatment, when Pol II is hyperphosphorylated but still not significantly degraded, minigene EDI exon inclusion is stimulated by severalfold (Figure 3E, left panel, dotted bar). Second, the UV effect is not affected by the proteasome inhibitor MG132 (Figure 3B, bottom). Third, Pol II ubiquitylation is performed by the E3 ubiquitin ligase activity present in the BRCA1/BARD1 complex (Kleiman et al., 2005; Xia et al., 2003), whose presence we showed to be unnecessary for the UV effect (Figure S2C).

CTD hyperphosphorylation caused by DNA damage can be the consequence of the activation of several kinases, including Cdk-7, Cdk-9, and Abelson tyrosine kinase (Abl). In an attempt to identify the kinase responsible for the UV effect, we treated the cells with different drugs. The Abl inhibitor PD166326 does not interfere with the effect of UV on AS (Figure S4A), in agreement with reports that UV treatment does not activate the Abl tyrosine kinase (Liu et al., 1996). On the other hand, the DNA-damaging agent doxorubicin that activates Abl has no effect on the AS reported here (Figure S4B). However, we found that the Cdk-9 inhibitor DRB (5,6-dichloro-1-β-D-ribofuranosylbenzimidazole) blocks the CTD hyperphosphorylation triggered by UV (Figure 3C). This not only confirms previous reports that UV activates Cdk-9 by causing dissociation of the inhibitory small nuclear RNA 7SK from the P-TEFb complex (Nguyen et al., 2001) but also suggests that the phosphorylation at Ser5 observed after UV treatment in Figure 3A might be performed by Cdk-9. Phosphorylation at Ser5 by Cdk-7 is usually associated with transcription initiation, whereas phosphorylation at Ser2 by Cdk-9 (a subunit of P-TEFb) is usually associated with the elongating form of Pol II. However, this might be an oversimplification, because it was shown that Ctdk-I, the yeast homolog to Cdk-9, can phosphorylate in vitro any of the two serines

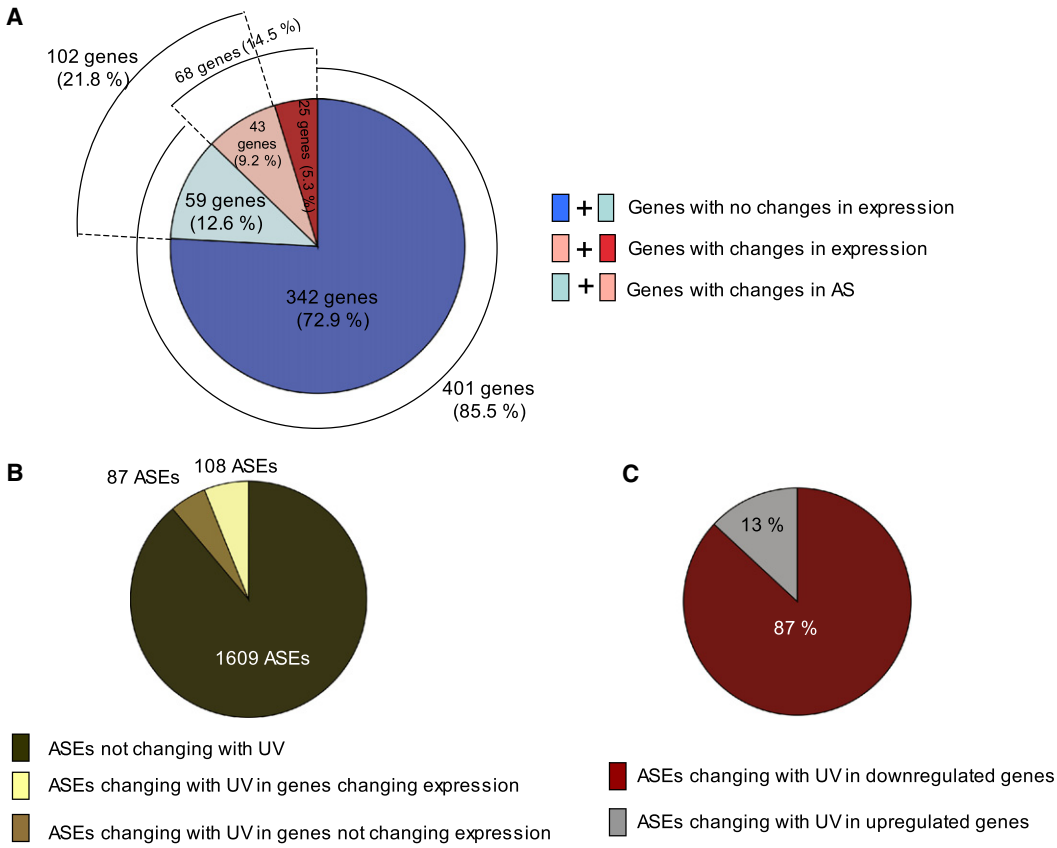

Figure 7. Splicing-Sensitive Human Microarray Analysis

(A) Distribution of genes that change expression, AS, or both in Hep3B cells, 6 hr after irradiation with 40 J/m^2 UV.

(B) Distribution of ASEs that change upon UV treatment corresponding to genes that change or do not change their expression.

(C) Distribution of ASEs that change upon UV treatment in upregulated and downregulated genes.

provided that the other one in the same heptad is already phosphorylated (Jones et al., 2004).

To determine if the hyperphosphorylation detected by western blot in the bulk of Pol II was also observed in the Pol II engaged in transcription, we performed chromatin immunoprecipitation (ChIP) analysis of a gene (*myc*) where Pol II distribution has been characterized in detail in one of our laboratories (Glover-Cutter et al., 2008). In agreement with the western blot results, UV treatment causes significant hyperphosphorylation of the DNA-associated Pol II at both serines along the *myc* gene between positions −39 and +4828 (Figure 3D).

Next, we wanted to correlate the time courses of Pol II hyperphosphorylation and the AS response. Figure 3E shows that endogenous AS responses to UV vary with the gene following a kinetics that, in all three cases, is subsequent to the hyperphosphorylation peak. The effect on endogenous FN EDI splicing, for example, is not seen until 16 hr after irradiation. However, and as mentioned above, the effect is observed much earlier with the tetracycline (Tet)-inducible FN minigene (3 hr, dotted bar), indicating that the 16 hr delay of the endogenous FN gene is probably the time needed to overcome the steady-state accumulation of the FN mRNA isoforms, whose half-lives are approximately 5 or 6 hr regardless of UV treatment (data not shown).

Different CTD Mutations Duplicate or Abrogate the UV Effect on AS

We reasoned that if the UV-induced hyperphosphorylation of Pol II was causing the change in AS, then a similar change should be seen with a mutant Pol II that mimics the hyperphosphorylated state, in the absence of UV. For this, we transfected the AS reporter minigene together with constructs expressing the large subunit of Pol II bearing either a wild-type (wt) CTD or CTDs where the serines at positions 2 or 5 were replaced by glutamic acids that mimic the effects of the phosphorylated serines. These polymerases carry an additional point mutation that confers α-amanitin resistance, enabling the inhibition of endogenous Pol II without affecting the transfected polymerases (de la Mata et al., 2003). Figure 4A shows that the replacement of either Ser2 or Ser5 by Glu (E2 and E5 mutants) stimulates EDI exon inclusion in two different cell lines, duplicating the effect of UV on AS. Consistently, when transcription in HCT116 cells is carried out by a Pol II CTD mutant with all its serines 2 and 5 replaced by alanines (Ala2 and Ala5 double mutant), no effect

of UV on AS is observed (Figure 4B), confirming that the UV effect is mediated by CTD hyperphosphorylation at serines 2 and 5.

DRB Blocks the UV Effect on AS

The alanine mutant experiment predicts that the inhibition of the UV-dependent CTD phosphorylation by DRB observed in Figure 3C should concomitantly abrogate the UV effect on AS. The difficulty with such an experiment is that DRB per se affects AS in certain cell lines and genes as it was shown for FN in Hep3B cells (Nogués et al., 2002). Fortunately, in HCT116 cells, DRB has little effect on basal FN EDI AS (Figure 4C, lanes 1 and 3), which is consistent with the negligible effect of the alanine mutant on basal EDI ratios (compare lanes 1 and 3 in Figure 4B). However, DRB clearly blocks the UV effect on AS (Figure 4C). The western blot at the bottom of Figure 4C certifies that DRB blocked basal and UV-dependent CTD phosphorylation in HCT116 cells. The basal AS patterns of Bcl-x and C9 are also affected by the phosphorylation status of the CTD because they are affected by DRB (Figure S5). These changes occur in the same direction as those caused by UV. Nevertheless, like in the case of EDI, DRB prevents the UV effect on Bcl-x and C9 AS. Together with the phosphomimetic and non-phosphorylatable CTD mutations, these experiments strengthen the causal relationship between CTD hyperphosphorylation and change in AS.

UV-Triggered DNA Damage Inhibits the Pol II Elongation Rate In Vivo

Because both Glu for Ser mutants have similar effects on AS, experiments in Figure 4A do not allow us to define which step of transcription is involved. To solve this problem, we decided to analyze the effect of UV on mRNA biogenesis in vivo and in real time using a MS2-GFP FRAP assay (Boireau et al., 2007; Darzacq et al., 2007). For this, cells expressing an HIV-1 reporter tagged with 24 binding sites for the MS2 phage protein (ExoLong cells, Boireau et al., 2007) were transfected with a construct expressing the MS2-GFP fusion protein and irradiated or not irradiated with UV at 40 J/m^2. The residency time of nascent mRNAs at their transcription sites was determined by photobleaching the MS2-GFP protein bound to RNA (Figure 5A). In untreated cells, recovery of MS2-GFP occurs in about 6 min. This curve has been previously interpreted with a two-step model (Boireau et al., 2007), containing an initial straight line that corresponds to elongation, followed by an exponential that accounts for 3′-end formation and transcript release (Figure 5B, green curve). One hour after exposure to UV, a similar curve is obtained, indicating no major alteration of mRNA biogenesis (red curve). However, 2 hr after UV treatment, recovery of MS2-GFP becomes markedly slower than the one observed in untreated cells (blue curve, 218 s for half-recovery against 123 s in untreated cells). Comparison of the untreated and 2 hr post-UV recovery curves reveals that their initial straight lines display the same slope up to the first 80 s following bleaching, but that UV-treated cells recovered more slowly after this time. Because elongation with the ExoLong template occurs during the first 148 s (Boireau et al., 2007), these results indicate that elongation is inhibited by the UV treatment. The inhibition of elongation is also supported by the fact that the FRAP behavior upon UV treatment is similar to the one observed when transcription is carried out by a slow Pol II mutant (Figure 5B, bottom).

An independent way of assessing the effects of UV on Pol II elongation is looking at total Pol II distribution along a gene by ChIP. UV treatment causes an 8-fold decrease in the amounts of Pol II detected at the *myc* promoter. However, if we normalize the +UV and −UV ChIP enrichments to 100% at the promoter region (position +1), the Pol II distribution on the *myc* gene in UV-treated cells shows an accumulation toward the promoter-proximal regions (Figure S6), consistent with an elongation defect.

In view of results in Figure 4A showing that the E2 and E5 CTD mutants duplicate the effects of UV on AS, we decided to investigate the elongation behavior of the E2 and E5 CTD mutants in vivo, using the MS2-GFP FRAP assay. The mutant polymerases were transiently transfected into the ExoShort cells (Boireau et al., 2007), together with MS2-GFP. The endogenous polymerases were inactivated by α-amanitin, and the remaining transcription sites were bleached. The recovery time of nascent RNAs transcribed by the E2 and E5 mutants were considerably longer than for the wt, α-amanitin-resistant control enzyme (WT^{res}) (Figure 5C). Indeed, half-recovery occurred in 78 s for the WT^{res} enzyme, but in 213 s and 270 s for the E2 and E5 mutants, respectively. This longer residency time of the nascent RNAs is mostly due to an increased time required for their transcription, rather than an altered 3′-end processing of the transcript. Elongation occurs during the first 60 s in ExoShort cells. At this time, the E2 and E5 mutants only recovered about half the signal generated by the wt enzyme (0.43 versus 0.25 and 0.21).

The UV/DRB Apparent Paradox

Interestingly, although UV and DRB have opposite effects on Pol II phosphorylation, both inhibit Pol II elongation in vivo (Figure 5 and Darzacq et al., 2007). We speculate that in certain situations persistent hyperphosphorylation (UV) or hypophosphorylation (DRB) might have similar consequences by interfering with the phosphorylation/dephosphorylation cycle needed for the concerted regulation of transcription initiation, elongation, termination, and reinitiation. An alternative explanation is that the CTD has at least two kinds of hyperphosphorylation states, both of which can be inhibited by DRB. It is conceivable that the CTD hyperphosphorylation state that inhibits elongation, such as the one provoked by treatment with UV and mimicked in the E2/E5 mutants, differs from the CTD hyperphosphorylation state of nonirradiated cells, characteristic of an elongating Pol II. It has been proposed that during elongation the CTD contains repeats phosphorylated at both Ser2 and Ser5 residues and that Ser5 phosphorylation decays, whereas Ser2 phosphorylation remains, toward the end of the gene. However, the Pol IIO band observed in western blots, like those in Figures 3A and 3C, does not necessarily contain a homogeneous population of molecules. The patterns of phosphorylation on individual Pol II CTDs can vary widely. This variation could be due to differential phosphorylation of Ser2 versus Ser5 and/or differential phosphorylation of the 52 repeats along the length of the CTD. Unfortunately, current methods do not permit an unequivocal assignment of the hyperphosphorylation patterns (Phatnani and

Greenleaf, 2006). The fact that the E2 and E5 mutations used in this work are present in all CTD repeats suggests that a homogeneous pattern of hyperphosphorylation could be the cause of lower elongation rates. In any case, results in Figure 5C indicate that individual replacements of Ser5 or Ser2 by Glu are sufficient to slow down elongation, which might suggest that an homogeneous phosphorylation at any of the two serines regulates elongation. These results reveal a much more complex picture compared to the accepted model of Ser5-P and Ser-2-P as landmarks of initiation and elongation, respectively. Inhibition of elongation by either DRB (Nogués et al., 2002 and Figure S5) or UV (Figure 1) affects AS in the same way in Hep3B cells, whereas in HCT116 cells DRB has little effect per se on EDI inclusion but clearly abrogates its stimulation by UV (Figure 4C). These results imply that additional cell-type-specific factors influence how CTD phosphorylation affects AS.

AS and UV-Induced Apoptosis in the Absence of p53

Because both the short Bcl-x and the long C9 isoform favor apoptosis, their increase after UV treatment might be physiologically relevant to prevent the eventual spreading of UV-induced, unrepaired mutations. Figure S5 indicates that the mechanism by which UV increases the proapoptotic/antiapoptotic isoform ratios of Bcl-x and C9 is similar to that of FN EDI and involves Pol II phosphorylation. A landmark of this effect is that it occurs in the absence of p53, a factor thought to be almost indispensable for the apoptotic response. Nevertheless, apoptosis is stimulated by UV treatment in the p53-null Hep3B cells in a dose-response manner, as revealed by the use of two different markers, caspase 3 (Figure 6A) and annexin V (Figure 6B). A role for Bcl-x in this apoptotic response is suggested by the negative correlation between the Bcl-x_L/Bcl-x_S ratio and the percentage of apoptotic cells upon increasing UV doses (Figure 6C). To determine if this correlation reflects causality, we investigated the effects of altering the Bcl-x_L/Bcl-x_S ratio by overexpressing the antiapoptotic long isoform (Bcl-x_L). For this, we used p53$^{-/-}$ HCT116 cells for their high transfection efficiency, needed for this experiment. Figure 6D shows that, like Hep3B cells, HCT p53$^{-/-}$ cells enter apoptosis with UV treatment (lanes 3 and 4), and this response is completely blocked by Bcl-x_L (lanes 5 and 6). This experiment demonstrates that the change induced by UV on Bcl-x AS is key for the p53-independent apoptotic response.

Splicing-Sensitive Microarrays

To assess the generality of the changes in transcription and AS, Hep3B cells were UV irradiated (or UV treated) with 40 J/m^2 UV and total RNA was isolated 6 hr later, reverse transcribed, labeled with Cy5 or Cy3 fluorochromes, and hybridized to a custom splicing-sensitive microarray (MA) as described in Supplemental Experimental Procedures.

The MA features 1804 AS events (ASEs) in 482 genes (Supplemental Spreadsheet 1), with probes covering both constitutive and alternative exons and exon-exon junctions. The distribution of the ASE types is illustrated in Figure S7A. Hybridization analysis revealed that 14.5% (68 genes) of the MA genes change their mRNA expression level upon UV treatment: among them, 78% (53 genes) were downregulated and 22% (15 genes) were upregulated. About 22% (102 genes) showed changes in at least one ASE with UV (Figure 7A). Most importantly, the proportion of genes that display AS is substantially higher among the genes evidencing changes in expression (43/68 genes, 63.2%) than among the genes that are not affected at the level of expression (59/401 genes, 14.7%). The genes that display AS changes upon UV exposure are listed in Table S2. Consistently, more ASEs change with UV among genes displaying gene expression changes (108 versus 87) (Figure 7B).

Another MA study (Pan et al., 2004) showed that, like global transcription profiles, global AS profiles reflect tissue identity. However, transcription and AS act independently on different sets of genes to define tissue-specific profiles, which seems in contrast with the significant fraction of genes showing changes in both expression and AS in our MAs. This apparent discrepancy might reflect that changes in gene transcription that define tissue-specific profiles (perhaps mostly quantitative) are not relevant for AS, whereas changes in the rate of transcription through the inhibition of elongation appear to be important for AS, particularly in a stress situation caused by DNA damage.

Our platform was designed to capture and to define in detail AS events of genes involved in cancer, cell cycle, cell proliferation, and cell death, and our results clearly demonstrate that several AS events of genes belonging to these functional categories changed upon UV treatment. Furthermore, an ontology analysis of the genes whose AS was affected by UV showed an enrichment in molecules involved in cell cycle, regardless of their transcriptional response (Figure S7B). As far as the ASEs studied individually in this paper, FN EDI and C9 are present in the array and changed consistently with UV either in the hybridization or in the validation. *myc* is also present and its expression is downregulated by UV consistently with the 8-fold decrease in Pol II recruitment to its promoter observed in ChIP.

Taken together, our data indicate that UV does not generally affect the level of either gene expression or AS, but its effects are restricted to a subset of responsive genes. However, the much higher proportion of ASE changes among genes changing gene expression and the predominance of downregulation (Figure 7C) are highly consistent with the mechanism described here.

Concluding Remarks

Inhibition of Pol II elongation has been shown to affect AS of many genes (de la Mata et al., 2003). In these cases, slowing down elongation is thought to favor the use of weak or suboptimal splice sites by increasing a time window opportunity for their recognition by the splicing machinery before downstream-stronger sites are synthesized. We show here that UV acts not only by specifying which genes are turned on and off but also by affecting transcription elongation and pre-mRNA processing decisions that in turn influence survival/death cell decisions. Our results reveal a CTD-dependent elongation response to DNA damage that slows down Pol II elongation, and show how a pathological environmental signal affects AS systemically, but not pleiotropically, through its coupling with transcription.

EXPERIMENTAL PROCEDURES

UV Treatment

UVC was performed using a CL-1000 ultraviolet crosslinker (UVP). Cells were first washed with phosphate-buffered saline and UV treatment was performed without cell medium, which was readded immediately after irradiation.

Transfections

Conditions for transfection of human hepatoma Hep3B and HCT116 cells with AS reporter minigenes driven by constitutive or Tet-inducible promoters were as described elsewhere (de la Mata et al., 2003).

RNA Preparation and Radioactive RT-PCR Analysis

RNA was purified using TRIzol reagent (Invitrogen). Radioactive reverse-transcriptase polymerase chain reaction (RT-PCR) of endogenous or minigene transfected EDI analysis were as described by de la Mata et al. (2003). Conditions and primers for Bcl-x and C9 PCR are described in Supplemental Experimental Procedures.

Pol II Expression Vectors

Conditions for expression of α-amanitin-resistant variants of the largest subunit of human Pol II (hRpb1) were as described elsewhere (de la Mata and Kornblihtt, 2006). The expression vectors for Rpb1 with mutant CTDs are based on pATRpb1 am^r.

Pol II ChIP

Pol II ChIP was carried out according to Glover-Cutter et al. (2008), using specific antibodies to P-Ser5 and P-Ser2 CTD epitopes therein described.

FRAP Analysis

U2OS-clone16 pExo-IRES-TK cells, transfections with vectors expressing MS2-GFP, and fluorescence analysis of the transcription sites on a wide-field microscope were as described previously (Boireau et al., 2007). Briefly, we used a Nikon TE200 equipped for both confocal and wide-field imaging (100×, NA 1.45). Transcription sites were bleached with the confocal port, using a circular region of 2.5 micron diameter (bleaching time, 1 s). Images were recorded with an EM-CCD camera (Cascade 512B, Roper) and a piezo-motor on the objective, to capture z-stacks every 3 to 12 s. For image analysis, fluorescence intensities were measured in a small parallelepiped (1 × 1 × 1.5 micron) placed at the most intense area of the transcription site. This allowed to track transcription sites in three dimensions and to correct for cell movements. Fluorescence intensities were normalized, and postbleach values were additionally set to zero.

Apoptosis Determination

Apoptosis was determined by two methods, annexin V or caspase 3 activity. For annexin V, apoptosis and necrosis secondary to apoptosis were assessed by annexin V and propidium iodide binding (Annexin-V Apoptosis Detection Kit, BD Biosciences, San Jose, CA, USA) and flow cytometric analysis (FACSCalibur, BD Biosciences) with at least 15,000 cells per point. Caspase 3 activity was determined by caspase 3 colorimetric protease assay (Invitrogen, catalog number KHZ0022) as described by the manufacturer.

SUPPLEMENTAL DATA

Supplemental Data contain Supplemental Experimental Procedures, seven figures, two tables, and one spreadsheet and can be found with this article online at http://www.cell.com/supplemental/S0092-8674(09)00270-0.

ACKNOWLEDGMENTS

We thank J. Wang for providing PD166326 and V. Gottifredi, S. Kim, M. Raíces, M. D'Angelo, R. Verdún, N. Lavagnino, V. Buggiano, G. Soria, and the members of the Srebrow and Kornblihtt labs for help and support. This work was supported by grants to A.R.K. from the Fundación Antorchas, the ANPCYT of Argentina, and the European AS Network (EURASNET); M.J.M., M.B., and M.d.l.M. are recipients of fellowships and A.R.K. is a career investigator of the CONICET. A.R.K. is an international research scholar of the Howard Hughes Medical Institute. Work in D.B.'s lab is supported by NIH grant GM58613. M.J.M. designed, performed, and interpreted the results of most experiments. M.S.P.S., M.d.l.M., M.B., and F.P. helped perform some experiments. S.B. and E.B. performed the FRAP experiments. G.B., K.G.C., and D.B. generated the CTD mutants and performed the ChIP experiments. M.P.P. and C.B-D. performed the microarray experiments. A.R.K. coordinated the work and prepared the manuscript.

Received: August 28, 2008
Revised: January 22, 2009
Accepted: March 2, 2009
Published: May 14, 2009

REFERENCES

Batsche, E., Yaniv, M., and Muchardt, C. (2006). The human SWI/SNF subunit Brm is a regulator of alternative splicing. Nat. Struct. Mol. Biol. *13*, 22–29.

Bentley, D.L. (2005). Rules of engagement: co-transcriptional recruitment of pre-mRNA processing factors. Curr. Opin. Cell Biol. *17*, 251–256.

Boireau, S., Maiuri, P., Basyuk, E., de la Mata, M., Knezevich, A., Pradet-Balade, B., Backer, V., Kornblihtt, A., Marcello, A., and Bertrand, E. (2007). The transcriptional cycle of HIV-1 in real-time and live cells. J. Cell Biol. *179*, 291–304.

Cáceres, J.F., and Kornblihtt, A.R. (2002). Alternative splicing: multiple control mechanisms and involvement in human disease. Trends Genet. *18*, 186–193.

Chandler, D.S., Singh, R.K., Caldwell, L.C., Bitler, J.L., and Lozano, G. (2006). Genotoxic stress induces coordinately regulated alternative splicing of the p53 modulators MDM2 and MDM4. Cancer Res. *66*, 9502–9508.

Cramer, P., Cáceres, J.F., Cazalla, D., Kadener, S., Muro, A.F., Baralle, F.E., and Kornblihtt, A.R. (1999). Coupling of transcription with alternative splicing: RNA pol II promoters modulate SF2/ASF and 9G8 effects on an exonic splicing enhancer. Mol. Cell *4*, 251–258.

Cui, R., Widlund, H.R., Feige, E., Lin, J.Y., Wilensky, D.L., Igras, V.E., D'Orazio, J., Fung, C.Y., Schanbacher, C.F., Granter, S.R., and Fisher, D.E. (2007). Central role of p53 in the suntan response and pathologic hyperpigmentation. Cell *128*, 853–864.

Damsma, G.E., Alt, A., Brueckner, F., Carell, T., and Cramer, P. (2007). Mechanism of transcriptional stalling at cisplatin-damaged DNA. Nat. Struct. Mol. Biol. *14*, 1127–1133.

Darzacq, X., Shav-Tal, Y., de Turris, V., Brody, Y., Shenoy, S.M., Phair, R.D., and Singer, R.H. (2007). In vivo dynamics of RNA polymerase II transcription. Nat. Struct. Mol. Biol. *14*, 796–806.

de la Mata, M., Alonso, C.R., Kadener, S., Fededa, J.P., Blaustein, M., Pelisch, F., Cramer, P., Bentley, D., and Kornblihtt, A.R. (2003). A slow RNA polymerase II affects alternative splicing in vivo. Mol. Cell *12*, 525–532.

de la Mata, M., and Kornblihtt, A.R. (2006). RNA polymerase II C-terminal domain mediates regulation of alternative splicing by SRp20. Nat. Struct. Mol. Biol. *13*, 973–980.

Efeyan, A., and Serrano, M. (2007). p53: guardian of the genome and policeman of the oncogenes. Cell Cycle *6*, 1006–1010.

Fededa, J.P., Petrillo, E., Gelfand, M.S., Neverov, A.D., Kadener, S., Nogues, G., Pelisch, F., Baralle, F.E., Muro, A.F., and Kornblihtt, A.R. (2005). A polar mechanism coordinates different regions of alternative splicing within a single gene. Mol. Cell *19*, 393–404.

Glover-Cutter, K., Kim, S., Espinosa, J., and Bentley, D.L. (2008). RNA polymerase II pauses and associates with pre-mRNA processing factors at both ends of genes. Nat. Struct. Mol. Biol. *15*, 71–78.

Hirose, Y., and Manley, J.L. (1998). RNA polymerase II is an essential mRNA polyadenylation factor. Nature *395*, 93–96.

Jones, J.C., Phatnani, H.P., Haystead, T.A., MacDonald, J.A., Alam, S.M., and Greenleaf, A.L. (2004). C-terminal repeat domain kinase I phosphorylates Ser2

and Ser5 of RNA polymerase II C-terminal domain repeats. J. Biol. Chem. *279*, 24957–24964.

Kadener, S., Cramer, P., Nogues, G., Cazalla, D., de la Mata, M., Fededa, J.P., Werbajh, S.E., Srebrow, A., and Kornblihtt, A.R. (2001). Antagonistic effects of T-Ag and VP16 reveal a role for RNA pol II elongation on alternative splicing. EMBO J. *20*, 5759–5768.

Karni, R., de Stanchina, E., Lowe, S.W., Sinha, R., Mu, D., and Krainer, A.R. (2007). The gene encoding the splicing factor SF2/ASF is a proto-oncogene. Nat. Struct. Mol. Biol. *14*, 185–193.

Katzenberger, R.J., Marengo, M.S., and Wassarman, D.A. (2006). ATM and ATR pathways signal alternative splicing of Drosophila TAF1 pre-mRNA in response to DNA damage. Mol. Cell. Biol. *26*, 9256–9267.

Kim, E., Magen, A., and Ast, G. (2007). Different levels of alternative splicing among eukaryotes. Nucleic Acids Res. *35*, 125–131.

Kleiman, F.E., and Manley, J.L. (2001). The BARD1-CstF-50 interaction links mRNA 3′ end formation to DNA damage and tumor suppression. Cell *104*, 743–753.

Kleiman, F.E., Wu-Baer, F., Fonseca, D., Kaneko, S., Baer, R., and Manley, J.L. (2005). BRCA1/BARD1 inhibition of mRNA 3′ processing involves targeted degradation of RNA polymerase II. Genes Dev. *19*, 1227–1237.

Kornblihtt, A.R., De La Mata, M., Fededa, J.P., Munoz, M.J., and Nogues, G. (2004). Multiple links between transcription and splicing. RNA *10*, 1489–1498.

Lazarev, D., and Manley, J.L. (2007). Concurrent splicing and transcription are not sufficient to enhance splicing efficiency. RNA *13*, 1546–1557.

Liu, Z.G., Baskaran, R., Lea-Chou, E.T., Wood, L.D., Chen, Y., Karin, M., and Wang, J.Y. (1996). Three distinct signalling responses by murine fibroblasts to genotoxic stress. Nature *384*, 273–276.

Luo, Z., Zheng, J., Lu, Y., and Bregman, D.B. (2001). Ultraviolet radiation alters the phosphorylation of RNA polymerase II large subunit and accelerates its proteasome-dependent degradation. Mutat. Res. *486*, 259–274.

Maniatis, T., and Reed, R. (2002). An extensive network of coupling among gene expression machines. Nature *416*, 499–506.

Nguyen, V.T., Kiss, T., Michels, A.A., and Bensaude, O. (2001). 7SK small nuclear RNA binds to and inhibits the activity of CDK9/cyclin T complexes. Nature *414*, 322–325.

Nicholls, C.D., Shields, M.A., Lee, P.W., Robbins, S.M., and Beattie, T.L. (2004). UV-dependent alternative splicing uncouples p53 activity and PIG3 gene function through rapid proteolytic degradation. J. Biol. Chem. *279*, 24171–24178.

Nogués, G., Kadener, S., Cramer, P., Bentley, D., and Kornblihtt, A.R. (2002). Transcriptional activators differ in their abilities to control alternative splicing. J. Biol. Chem. *277*, 43110–43114.

Pan, Q., Shai, O., Misquitta, C., Zhang, W., Saltzman, A.L., Mohammad, N., Babak, T., Siu, H., Hughes, T.R., Morris, Q.D., et al. (2004). Revealing global regulatory features of mammalian alternative splicing using a quantitative microarray platform. Mol. Cell *16*, 929–941.

Phatnani, H.P., and Greenleaf, A.L. (2006). Phosphorylation and functions of the RNA polymerase II CTD. Genes Dev. *20*, 2922–2936.

Robson-Dixon, N.D., and Garcia-Blanco, M.A. (2004). MAZ elements alter transcription elongation and silencing of the fibroblast growth factor receptor 2 exon IIIb. J. Biol. Chem. *279*, 29075–29084.

Rockx, D.A., Mason, R., van Hoffen, A., Barton, M.C., Citterio, E., Bregman, D.B., van Zeeland, A.A., Vrieling, H., and Mullenders, L.H. (2000). UV-induced inhibition of transcription involves repression of transcription initiation and phosphorylation of RNA polymerase II. Proc. Natl. Acad. Sci. USA *97*, 10503–10508.

Schwerk, C., and Schulze-Osthoff, K. (2005). Regulation of apoptosis by alternative pre-mRNA splicing. Mol. Cell *19*, 1–13.

Shomron, N., Alberstein, M., Reznik, M., and Ast, G. (2005). Stress alters the subcellular distribution of hSlu7 and thus modulates alternative splicing. J. Cell Sci. *118*, 1151–1159.

Skorski, T. (2002). BCR/ABL regulates response to DNA damage: the role in resistance to genotoxic treatment and in genomic instability. Oncogene *21*, 8591–8604.

Somesh, B.P., Reid, J., Liu, W.F., Sogaard, T.M., Erdjument-Bromage, H., Tempst, P., and Svejstrup, J.Q. (2005). Multiple mechanisms confining RNA polymerase II ubiquitylation to polymerases undergoing transcriptional arrest. Cell *121*, 913–923.

van der Houven van Oordt, W., Diaz-Meco, M.T., Lozano, J., Krainer, A.R., Moscat, J., and Cáceres, J.F. (2000). The MKK(3/6)-p38-signaling cascade alters the subcellular distribution of hnRNP A1 and modulates alternative splicing regulation. J. Cell Biol. *149*, 307–316.

Xia, Y., Pao, G.M., Chen, H.W., Verma, I.M., and Hunter, T. (2003). Enhancement of BRCA1 E3 ubiquitin ligase activity through direct interaction with the BARD1 protein. J. Biol. Chem. *278*, 5255–5263.